PERGAMON

Neural Networks 14 (2001) 381–393

Neural Networks

www.elsevier.com/locate/neunet

Contributed article

Quantitative examinations for multi joint arm trajectory planning—using a robust calculation algorithm of the minimum commanded torque change trajectory

Yasuhiro Wada[a,*], Yuichi Kaneko[a], Eri Nakano[b], Rieko Osu[c], Mitsuo Kawato[c,d]

[a]Nagaoka University of Technology, 1603-1 Kamitomioka, Nagaoka-shi, Niigata, 940-2188, Japan
[b]Advanced Telecommunication Research Laboratories, Kyoto, 619-0288, Japan
[c]ERATO Dynamic Brain Project, Kyoto, 619-0288, Japan
[d]ATR Human Information Processing Research Laboratories, Kyoto, 619-0288, Japan

Received 23 March 2000; revised 26 December 2000; accepted 26 December 2000

Abstract

In previous research, criteria based on optimal theories were examined to explain trajectory features in time and space in multi joint arm movement. Four criteria have been proposed. They were the minimum hand jerk criterion (by which a trajectory is planned in an extrinsic-kinematic space), the minimum angle jerk criterion (which is planned in an intrinsic-kinematic space), the minimum torque change criterion (where control objects are joint links; it is planned in an intrinsic-dynamic-mechanical space), and the minimum commanded torque change criterion (which is planned in an intrinsic space considering the arm and muscle dynamics). Which of these is proper as a criterion for trajectory planning in the central nervous system has been investigated by comparing predicted trajectories based on these criteria with previously measured trajectories. Optimal trajectories based on the two former criteria can be calculated analytically. In contrast, optimal trajectories based on the minimum commanded torque change criterion are difficult to be calculated, even with numerical methods. In some cases, they can be computed by a Newton-like method or a steepest descent method combined with a penalty method. However, for a realistic physical parameter range, the former becomes unstable quite often and the latter is unreliable about the optimality of the obtained solution.

In this paper, we propose a new method to stably calculate optimal trajectories based on the minimum commanded torque change criterion. The method can obtain trajectories satisfying Euler–Poisson equations with a sufficiently high accuracy. In the method, a joint angle trajectory, which satisfies the boundary conditions strictly, is expressed by using orthogonal polynomials. The coefficients of the orthogonal polynomials are estimated by using a linear iterative calculation so as to satisfy the Euler–Poisson equations with a sufficiently high accuracy. In numerical experiments, we show that the optimal solution can be computed in a wide work space and can also be obtained in a short time compared with the previous methods.

Finally, we perform supplementary examinations of the experiments by Nakano, Imamizu, Osu, Uno, Gomi, Yoshioka et al. (1999). Estimation of dynamic joint torques and trajectory formation from surface electromyography signals using a neural network model. *Biological Cybernetics*, *73*, 291–300. Their experiments showed that the measured trajectory is the closest to the minimum commanded torque change trajectory by statistical examination of many point-to-point trajectories over a wide range in a horizontal and sagittal work space. We recalculated the minimum commanded torque change trajectory using the proposed method, and performed the same examinations as previous investigations. As a result, it could be reconfirmed that the measured trajectory is closest to the minimum commanded torque change trajectory previously reported. © 2001 Elsevier Science Ltd. All rights reserved.

Keywords: Minimum commanded torque change criterion; Euler–Poisson equation; Orthogonal polynomial; Trajectory planning; Optimization

1. Introduction

The following two characteristics have been well demonstrated about the feature of a point-to-point human arm movement on a plane (Abend, Bizzi, & Morasso, 1982). (1) The path is a roughly straight line, but is slightly curved. (2) The velocity profile is bell shaped with a single peak. Several models have been proposed to explain these features (Bizzi, Accornero, Chapple, & Hogan, 1984; Flash & Hogan, 1985; Nakano, Imamizu, Osu, Uno, Gomi, Yoshioka et al., 1999; Rosenbaum, Loukopoulos, Meulenbroek, Vaughan, & Engelbrecht, 1995; Uno, Kawato, & Suzuki, 1989). In particular, the following criteria for trajectory planning based on optimal principles have been proposed.

The minimum hand jerk criterion (Flash & Hogan, 1985)

* Corresponding author. Fax: +81-258-47-9500.
E-mail address: ywada@nagaokaut.ac.jp (Y. Wada).

PII: S0893-6080(01)00026-0

is planned in an extrinsic-kinematic space, the minimum angle jerk criterion is planned in an intrinsic-kinematic space (Rosenbaum et al., 1995), the minimum torque change criterion (Uno et al., 1989), where control objects are joint links, is planned in an intrinsic-dynamic-mechanical space, and the minimum commanded torque change criterion (Nakano et al., 1999) is planned in an intrinsic space considering the arm and muscle dynamics and using representations for motor commands controlling the muscle tensions. The former two criteria are planned in a kinematic space, and the latter two criteria are models that depend on the dynamics of the arm. The final target in this paper is to discuss which of these trajectory planning criteria based on optimal principles is appropriate as a criterion for trajectory planning in the central nervous system.

Incidentally, analytical solutions for the minimum hand jerk criterion and the minimum angle jerk criterion can be calculated easily. However, the latter two models, which smoothen the change of the torque or the commanded torque, must be solved under several constraints with the nonlinear dynamics and boundary conditions at the starting and final points. That is, we have to solve a nonlinear, optimization problem.

In general, it is quite difficult to obtain an optimal solution. Nakano et al. (1999); Sakuraba, Osu, Nakano, Wada, and Kawato (2000) reported that the trajectory predicted by the minimum commanded torque change criterion is the trajectory closest to a human trajectory among trajectories predicted by the above criteria. However, it has been very difficult to establish a robust method for obtaining an optimal trajectory based on the minimum commanded torque change criterion at various starting points, final points, and dynamic parameters. The optimal trajectory can be obtained by the Newton-like method (Uno et al., 1989), and the steepest descent method (Nakano et al., 1999). The Newton-like method is an algorithm to guarantee the local optimality of the converged trajectory mathematically; however, the algorithm often becomes unstable according to the parameter value of the dynamics such as the viscosity, and then, often diverges. The algorithm also occasionally diverges according to the positions of the starting and final points. On the other hand, the optimal solution can be stable and computed comparatively more easily using the steepest descent method. However, the optimality of the solution cannot be guaranteed. Because it was difficult for Nakano et al. (1999) to calculate an optimal trajectory of the minimum commanded torque change, comparisons were made on quasi-optimal trajectories based on the minimum commanded torque change obtained using the steepest descent method and measured trajectories.

Calculating the optimal trajectory is necessary and indispensable for explaining human arm movements by a mathematical model. Therefore, the need is high for an algorithm that can calculate the optimal trajectory accurately and without fail based on the minimum commanded torque change criterion, regardless of the positions of the starting and final points or the value of the dynamic parameter.

In this paper, first of all, we propose a trajectory calculation method based on the minimum commanded torque change criterion, which satisfies Euler–Poisson equations with a sufficiently high accuracy. These Euler–Poisson equations, which are derived from the functional optimal problem, provide the necessary condition for obtaining the optimal trajectory. In the proposed method, the joint angle trajectory is expressed by a system of orthogonal polynomials for time, and each coefficient of the orthogonal polynomials is estimated by using a linear, iterative operation to satisfy the Euler–Poisson equations as much as possible. We show the numerical experiment results of the minimum commanded torque change trajectory generation for a two-joint arm on two planes (the horizontal and sagittal planes) and also point out that the optimal trajectory, which satisfies the Euler–Poisson equations with a sufficiently high accuracy, can be obtained in a short time, regardless of the positions of the starting and final points or the value of the dynamic parameter. Finally, we discuss the adequacy of the trajectory planning criterion. We examine four trajectory planning criteria in multi joint reaching movements, which can explain the universal features in arm trajectories well, as mentioned above, quantitatively and statistically using many movement trajectories measured on various and not local spaces (Nakano et al.,1999).

2. Optimal criteria for trajectory planning and calculation algorithm

2.1. Minimum hand jerk criterion

With the minimum hand jerk criterion (Flash & Hogan, 1985) a trajectory is planned according to the arm position (x, y) in an extrinsic-kinematic space given from vision independently of the musculoskeletal dynamics. The trajectory is planned so as to minimize the time integral of jerk (three times differentiation of the hand position with respect to time). The objective function is given as follows:

$$C_J = \frac{1}{2}\int_0^{t_f}\left\{\left(\frac{d^3x}{dt^3}\right)^2 + \left(\frac{d^3y}{dt^3}\right)^2\right\}dt \tag{1}$$

Here, t_f shows the duration.

In a point-to-point movement, the trajectory predicted by the criterion is a straight line trajectory in the Cartesian coordinate. The tangential velocity is a bell shape with a single peak. Flash and Hogan (1985) claimed that the minimum hand jerk criterion can reproduce a trajectory corresponding well with movement data from human subjects. An attractive point is that the analytical optimal trajectory, which satisfies the minimum hand jerk trajectory, can be obtained easily.

$$x^{\mathrm{J}}(t) = x^{\mathrm{s}} + (x^{\mathrm{s}} - x^{\mathrm{f}})\left(-10\left(\frac{t}{t_f}\right)^3 + 15\left(\frac{t}{t_f}\right)^4 - 6\left(\frac{t}{t_f}\right)^5\right) \quad (2)$$

$$y^{\mathrm{J}}(t) = y^{\mathrm{s}} + (y^{\mathrm{s}} - y^{\mathrm{f}})\left(-10\left(\frac{t}{t_f}\right)^3 + 15\left(\frac{t}{t_f}\right)^4 - 6\left(\frac{t}{t_f}\right)^5\right) \quad (3)$$

Here, x^{s}, y^{s} and x^{f}, y^{f} correspond to the position of the starting point and the position of the final point, respectively.

2.2. Minimum angle jerk criterion

A trajectory based on the minimum angle jerk criterion is planned so as to minimize the change of the angle acceleration. That is, the object function of the minimum angle jerk criterion is expressed by minimizing the integration of the jerk over the motion duration, as shown in Eq. (4):

$$C_{\mathrm{AJ}} = \frac{1}{2}\int_0^{t_f}\sum_{i=1}^{2}\left(\frac{\mathrm{d}^3\theta_i}{\mathrm{d}t^3}\right)^2 \mathrm{d}t \quad (4)$$

θ_i shows the joint angle of joint i here. An analytical solution of the criterion can be easily obtained in the same manner as the minimum hand jerk model. The minimum angle jerk trajectory is expressed as the following equations, which are the fifth spline functions.

$$\theta_i^{AJ}(t) = \theta_i^s + (\theta_i^s - \theta_i^f)\left(-10\left(\frac{t}{t_f}\right)^3 + 15\left(\frac{t}{t_f}\right)^4 - 6\left(\frac{t}{t_f}\right)^5\right)$$

$$(0 \le t \le t_f) \quad (5)$$

Here, θ_i^{s} and θ_i^{f} show the joint angle at the starting point and the final point of joint i, respectively. The trajectory predicted by the criterion is independent of the influence of the arm dynamics and the motion duration, except the arm length. The point-to-point movement trajectory planned by the criterion is a straight path in the joint space. The trajectory transformed in the Cartesian coordinate is gradually curved according to the arm position.

2.3. Minimum torque change criterion

The minimum torque change trajectory is planned so that the change of torque τ generated by each joint becomes the smallest. The object function is given by the following equation:

$$C_{\mathrm{TC}} = \frac{1}{2}\int_0^{t_f}\sum_{i=1}^{2}\left(\frac{\mathrm{d}\tau_i}{\mathrm{d}t}\right)^2 \mathrm{d}t \quad (6)$$

τ_i shows the torque generated by joint i. The minimum torque change criterion (Uno et al., 1989) depends on the arm dynamics. The minimum torque change criterion can reproduce the gradually curved trajectory unable to be explained by the minimum hand jerk criterion. Moreover, movements that pass via points and movements to which an external force is applied can be reproduced. The torque is calculated from an equation of two link manipulators (Eq. (7)).

$$\begin{aligned}\tau_1 = \{&I_1 + I_2 + 2M_2L_1S_2\cos\theta_2 + M_2(L_1)^2\}\ddot{\theta}_1 + (I_2 \\ &+ M_2L_1S_2\cos\theta_2)\ddot{\theta}_2 - M_2L_1S_2(2\dot{\theta}_1 + \dot{\theta}_2)\dot{\theta}_2\sin\theta_2 \\ &+ B_{11}\dot{\theta}_1 + B_{12}\dot{\theta}_2 + g\{(M_1S_1 + M_2L_1)\sin\theta_1 \\ &+ M_2S_2\sin(\theta_1 + \theta_2)\}\end{aligned}$$

$$\begin{aligned}\tau_2 = &(I_2 + M_2L_1S_2\cos\theta_2)\ddot{\theta}_1 + I_2\ddot{\theta}_2 + M_2L_1S_2(\dot{\theta}_1)^2\sin\theta_2 \\ &+ B_{22}\dot{\theta}_2 + B_{21}\dot{\theta}_1 + gM_2S_2\sin(\theta_1 + \theta_2)\end{aligned} \quad (7)$$

Here, τ_1 and θ_1 show the torque and the joint angle of the shoulder, and τ_2 and θ_2 show the torque and joint angle of the elbow, respectively. I_i, M_i, L_i, and S_i, show the inertia moment surroundings of link i ($i = 1, 2$), mass, arm length, and the distance from the position of the joint to the position of the center of the gravity. The three-dimensional shape of a male's arm was measured by a Cyberware Laser Range Scanner. We calculated the arm as a homogeneous material with a specific gravity of 1.0 and computed its mass, center of mass, and moment of inertia from its volume. The arm parameters for each subject were calculated using the ratio of the arm length based on the measured data. B_{ij} shows the viscosity coefficient expressing the influence of the angular velocity of joint j on the torque of joint i. Links 1 and 2 correspond to the upper arm and the forearm. Moreover, g is the acceleration of gravity. The term concerning g shows the force supporting the arm. Therefore, g is set to 0 for movement in the horizontal plane. Incidentally, in the minimum torque change model proposed by Uno et al. (1989), only the link dynamics is regarded as the controlled object.

The minimum torque change trajectory is extremely sensitive to the value of the viscosity. Most of the viscosity measured around a joint is ascribed to a biochemical and mechanical reaction process within the muscle when it receives impulses and generates tension, which is not ascribed to a passive property of the joint (Akazawa, 1994). Considering the viscosity in calculating the torque means that both the link dynamics and muscle are regarded as controlled objects. It is not appropriate to use a non-zero viscous value to calculate the torque because the literal minimum torque change model takes the actual torque around the joint as an object for optimization (Flash, 1990). Therefore, the actual torque with zero viscosity $B_{ij} = 0$ is calculated from the dynamics equation of a two-link manipulation.

2.4. Minimum commanded torque change criterion

Even if the hand position is determined in the extrinsic coordinates, the joint angles or the muscle lengths cannot be uniquely determined because of redundant degrees of freedom. When a desired trajectory is determined in the joint angle coordinate, the actual torques around the joints can be calculated by an inverse dynamics equation. However, there are also an infinite number of possible combinations of agonist and antagonist muscle tensions that can generate the same torques. The degrees of freedom of α-motoneurons, which innervate each muscle, are higher than those of the muscles, and cortical motor neurons may have higher degrees of freedom than α-motoneurons. Even if the time profiles of muscle tensions are specified, the firing rates of the cortex or spinal cord neurons cannot be uniquely determined. Regardless of these indeterminacies, the actual hand trajectories show common invariant characteristics, and electromyographic (EMG) signals appear in typical triphasic patterns. These observations suggest that the brain solves these ill-posed problems based on some principles.

The minimum motor command change model (Kawato, 1992, 1996) has been proposed for trajectory planning in an intrinsic-dynamic-neural space. The minimum angle jerk criterion and the minimum torque change criterion can be calculated from a comparatively easy physical parameter. Because the minimum motor command change model can conceptualize signals at the α-motoneuron or cortical motoneuron level, all indeterminacies can be constrained at each level. Although an attempt has been made to estimate the motor commands at the muscle level (Koike & Kawato, 1995), it is extremely difficult to estimate the motor commands of the spinal cord or cortex by modeling the information processing from a central system to a peripheral system.

A quantitative model, not a conceptual model, is needed to actually compute an optimal trajectory. Therefore, first, a minimum commanded torque change model that approximates the minimum motor command change model and has computability is proposed, while positively appreciating the assumption of non-zero viscosity by Uno et al. (1989). In the literal minimum torque change model, only the link dynamics is regarded as the controlled object, whereas the minimum commanded torque change model, both the link dynamics and muscles are regarded as controlled objects. We employ motor commands at the peripheral level, in other words, we use signals controlling muscle tensions to model the minimum commanded torque change criterion. In terms of indeterminacy, however, the minimum commanded torque change model solves problems at the same level, that is, the torque level as the minimum torque change model.

With the minimum commanded torque change criterion, the link dynamics and the muscles are controlled, and the trajectory is planned so as to minimize the time integral of the square of the commanded torque change rate. The object function is conceptually different though is given by an expression identical to the minimum torque change criterion as Eq. (8) shows,

$$C_{\mathrm{CTC}} = \frac{1}{2}\int_0^{t_f}\sum_{i=1}^{N}\left(\frac{\mathrm{d}\tau_i^c}{\mathrm{d}t}\right)^2 \mathrm{d}t \tag{8}$$

Here, t_f indicates the movement time, and N shows the number of joints. τ^{c} shows the commanded torque. Incidentally, the commanded torque does not correspond to the mechanical output torque. It is an approximated torque for the motor commands. A point-to-point movement based on the criterion is planned in consideration of the dynamics parameters of the mass of the arm and the inertia movement, etc., shown in Eq. (7). The feature of the trajectory generated by the criterion changes according to the start posture and final posture.

In this paper, Eq. (7) for a two-link, two-joint arm was used for the calculation of the commanded torque. It was extremely difficult to predict a trajectory satisfying the criterion as well as the minimum torque change criterion. In particular, because the value of the viscosity was not set to 0 for the minimum commanded torque change criterion, it became more difficult to obtain the solution by the Newton-like method.

In our study, we use the following formula, which was estimated from the actual torque and viscosity during static force control (Gomi & Osu, 1998), to acquire viscous values of diagonal components (B_{11}, B_{22}) and off-diagonal components (B_{21}, B_{12}) for each trajectory. Here, for simplicity, mean absolute torques (shoulder:τ_1^{ma} , elbow:τ_2^{ma}) during movement are used as the actual torques.

$$\begin{aligned}[B_{11}, B_{12}(=B_{21}), B_{22}] = [&0.63 + 0.095\tau_1^{\mathrm{ma}},\\ &0.175 + 0.0375\tau_2^{\mathrm{ma}}, 0.76 + 0.185\tau_2^{\mathrm{ma}}] \quad \mathrm{Nm/(rad/s)}\end{aligned} \tag{9}$$

We propose a new method to calculate the minimum commanded torque change trajectory, which is based on the Euler–Poisson equation and can predict an optimal trajectory robust for the change of the value of the dynamics parameter such as a viscosity. Naturally, the method can also be applied to the minimum torque change criterion.

3. A prediction algorithm for trajectories based on the minimum commanded torque change criterion using the Euler–Poisson equation

3.1. Euler–Poisson equation

In this section, a calculation algorithm for trajectories based on the minimum commanded torque change criterion using the Euler–Poisson equation is described. Basically, the algorithm calculates a trajectory that satisfies the

Euler–Poisson equations with a high accuracy and the boundary conditions strictly. The object function of the minimum commanded torque change criterion (Eq. (8)) is expressed as follows.

$$C_{\mathrm{CTC}} = \frac{1}{2}\int_0^{t_f} F(t, \theta_1, \theta_2, \dot{\theta}_1, \dot{\theta}_2, \ddot{\theta}_1, \ddot{\theta}_2, \theta_1^{(3)}, \theta_2^{(3)})\mathrm{d}t \to \mathrm{Min} \tag{10}$$

Here, $F = \sum_{i=1}^{2}\left(\mathrm{d}\tau_i^{\mathrm{c}}/\mathrm{d}t\right)^2$, $\theta_1^{(3)}$ and $\theta_2^{(3)}$ show the differential coefficient of the third order with respect to the time of θ_1 and θ_2, respectively. By the boundary conditions of the starting point and the final point (position, velocity, and acceleration), the following Euler–Poisson equations for the above optimal problem can be derived as a necessary condition for an extreme value.

$$E_1 = \frac{\partial}{\partial\theta_1}F - \frac{\mathrm{d}}{\mathrm{d}t}\frac{\partial}{\partial\dot{\theta}_1}F + \frac{\mathrm{d}^2}{\mathrm{d}t^2}\frac{\partial}{\partial\ddot{\theta}_1}F - \frac{\mathrm{d}^3}{\mathrm{d}t^3}\frac{\partial}{\partial\theta_1^{(3)}}F = 0$$

$$E_2 = \frac{\partial}{\partial\theta_2}F - \frac{\mathrm{d}}{\mathrm{d}t}\frac{\partial}{\partial\dot{\theta}_2}F + \frac{\mathrm{d}^2}{\mathrm{d}t^2}\frac{\partial}{\partial\ddot{\theta}_2}F - \frac{\mathrm{d}^3}{\mathrm{d}t^3}\frac{\partial}{\partial\theta_2^{(3)}}F = 0 \tag{11}$$

Therefore, θ_1 and θ_2, which satisfy these two Euler–Poisson equations for every movement time, are the minimum commanded torque change trajectory.

3.2. A system of orthogonal polynomials for expression of the minimum commanded torque change trajectory

The minimum angle jerk trajectory is one of the good approximations of the minimum commanded torque change trajectory. Here, let us assume that the minimum commanded torque change trajectory $\theta_i(t)$ $(i = 1, 2)$ can be expressed by the following equation.

$$\theta_i(t) = \theta_i^{\mathrm{AJ}}(t) + \Delta\theta_i(t) \tag{12}$$

Here, $\theta_i^{\mathrm{AJ}}(t)$ corresponds to the minimum angle jerk trajectory, and $\Delta\theta_i(t)$ is denoted as the difference between the minimum commanded torque change trajectory and the minimum angle jerk trajectory. The trajectory of Eq. (12) must satisfy the following boundary conditions of the starting position and final position.

$$\begin{aligned} &\theta_i(0) = \theta_i^{\mathrm{s}}, \qquad \dot{\theta}_i(0) = \ddot{\theta}_i(0) = 0, \\ &\theta_t(t_f) = \theta_i^{\mathrm{f}}, \qquad \dot{\theta}_i(t_f) = \ddot{\theta}_i(t_f) = 0 \qquad (i = 1, 2) \end{aligned} \tag{13}$$

In the next section, we show concrete equations of the minimum angle jerk trajectory and the second term on the right side of Eq. (12).

3.2.1. A difference trajectory $\Delta\theta_i(t)$

$\theta_i^{\mathrm{AJ}}(t)$ in Eq. (12) is the minimum angle jerk trajectory, which satisfies the boundary conditions (Eq. (13)). Therefore, $\Delta\theta_i(t)$ should be a function that makes the boundary conditions at the starting point and final point all become 0. We use the Jacobian polynomial (Szego, 1975) as the set of orthogonal polynomials to express $\Delta\theta_i(t)$ (see Appendix A). The Jacobian polynomial can be represented as $\tilde{Q}_k(t) = 64t^3(1-t)^3\tilde{P}_k^{(6,6)}(t)$. We define the difference trajectory $\Delta\theta_i(t)$ as the following equations, which are normalized to $0 \le t \le 1$.

$$\Delta\theta_i(t) = \sum_k 64 a_{ik} t^3 (1-t)^3 \tilde{P}_k^{(6,6)}(t) \tag{14}$$

$\Delta\theta_i(t)$ is composed of the summation of Jacobian orthogonal polynomials; the boundary conditions of the position, velocity, and acceleration at the starting point and final point all satisfy 0. From the above, the minimum commanded torque change trajectory $\theta_i(t)$ is given by Eq. (15).

$$\theta_i(t) = \theta_i^{\mathrm{s}} + (\theta_i^{\mathrm{s}} - \theta_i^{\mathrm{f}})(-10t^3 + 15t^4 - 6t^5) + 64t^3(1 - t)^3 \sum_{k=0}^{K} a_{ik}\tilde{P}_k^{(6,6)}(t) \tag{15}$$

Jacobian polynomials $P_{k+1}^{(6,6)}(x)$ obtained by a recurrence formula from the first to the $(k+1)$th order are shown in Appendix A.

3.3. An estimation algorithm of parameter a_{ik}

To estimate a_{ik} satisfying the Euler–Poisson equations with a high accuracy, we propose the following two innovations. (1) The left side of the Euler–Poisson equation is expressed as a linear summation concerning a_{ik}, and (2) the coefficient a_{ik} is estimated using an iterative calculation by the discretization of the movement time.

3.3.1. A linear summation concerning parameter a_{ik}

Eq. (15) is substituted for Eq. (11), and this is arranged to become a linear expression of a_{ik} such as Eq. (16).

$$\begin{aligned} &E_1(t, \theta_1, \theta_2, \dot{\theta}_1, \dot{\theta}_2, \ldots, \theta_1^{(3)}, \theta_2^{(3)}) \\ &= \sum_{i=1}^{2}\sum_{k=0}^{K} {}_1h_{ik}(t, \theta_1, \theta_2, \dot{\theta}_1, \dot{\theta}_2, \ddot{\theta}_1, \ddot{\theta}_2)a_{ik} \\ &\quad + J_1(t, \theta_1, \theta_2, \dot{\theta}_1, \dot{\theta}_2, \ldots, \theta_1^{(3)}, \theta_2^{(3)}) \\ &E_2(t, \theta_1, \theta_2, \dot{\theta}_1, \dot{\theta}_2, \ldots, \theta_1^{(3)}, \theta_2^{(3)}) \\ &= \sum_{i=1}^{2}\sum_{k=1}^{K} {}_2h_{ik}(t, \theta_1, \theta_2, \dot{\theta}_1, \dot{\theta}_2, \ddot{\theta}_1, \ddot{\theta}_2)a_{ik} \\ &\quad + J_2(t, \theta_1, \theta_2, \dot{\theta}_1, \dot{\theta}_2, \ldots, \theta_1^{(3)}, \theta_2^{(3)}) \end{aligned} \tag{16}$$

Eq. (16) is obtained according to the standard of the following (A) and (B).

(A) Terms $[1, A_1, A_2]\cdot\theta_i^{(n)}$

Here, [ ] $\theta_i^{(n)}$ indicate product terms of the inside

Table 1
Terms in ${}_1h_{ik}$, ${}_2h_{ik}$, J_1, and J_2

${}_1h_{ik}$, ${}_2h_{ik}$	Sum of A_1 term[a]
	Sum of A_2, B_1, $[A_2, A_3]\cdot B_1$ terms
J_1, J_2	Sum of B_2, $[A_1, A_4]\cdot B_2$ terms[a]
	Sum of B_3, $[A_2, A_3]\cdot B_3$ terms
A_1	$\cos(\theta_1), \cos(\theta_1+\theta_2), \cos^2(\theta_1), \cos^2(\theta_1+\theta_2), \cos(\theta_1)\cos(\theta_2), \cos(\theta_1)\cos(\theta_1+\theta_2), \cos(\theta_2)\cos(\theta_1+\theta_2)$
A_2	$\cos(\theta_2)$, $\cos 2(\theta_2)$
A_3	$\sin(\theta_2)$, $\sin 2(\theta_2)$, $\sin(\theta_2)\cos(\theta_2)$
A_4	$\sin(\theta_1), \sin(\theta_1+\theta_2), \sin(\theta_1)\cos(\theta_1), \sin(\theta_1)\cos(\theta_1+\theta_2), \cos(\theta_1)\sin(\theta_1+\theta_2), \sin(\theta_1)\sin(\theta_2), \sin(\theta_1)\cos(\theta_2), \cos(\theta_1)\sin(\theta_2), \sin(\theta_2)\sin(\theta_1+\theta_2),$ $\sin(\theta_2)\cos(\theta_1+\theta_2), \cos(\theta_2)\sin(\theta_1+\theta_2), \sin(\theta_1+\theta_2)\cos(\theta_1+\theta_2)$
B_1	$\theta_{\mathrm{i}}^{(1)}, \theta_2^{(1)}, (\theta_1^{(1)})^2, (\theta_2^{(1)})^2, \theta_1^{(1)}\theta_2^{(1)}$
B_2	$(\theta_1^{(1)})^2$, $(\theta_2^{(1)})^2$, $\theta_1^{(1)}\theta_2^{(1)}$, $(\theta_1^{(1)})^3$, $(\theta_2^{(1)})^3$, $(\theta_1^{(1)})^2\theta_2^{(1)}$, $\theta_1^{(1)}(\theta_2^{(1)})^2$, $(\theta_1^{(1)})^4$, $(\theta_2^{(1)})^4$, $(\theta_1^{(1)})^3\theta_2^{(1)}$, $\theta_1^{(1)}(\theta_2^{(1)})^3$, $(\theta_1^{(1)})^2(\theta_2^{(1)})^2$, $(\theta_1^{(2)})^2$, $\theta_2^{(2)})^2$, $\theta_1^{(2)}\theta_2^{(2)}$, $(\theta_1^{(1)})^2\theta_1^{(2)}$, $\theta_1^{(2)}(\theta_2^{(1)})^2$, $\theta_1^{(1)}\theta_1^{(2)}$, $\theta_2^{(1)}\theta_1^{(2)}$, $\theta_1^{(1)}\theta_2^{(2)}$, $\theta_2^{(1)}\theta_2^{(2)}$, $\theta_1^{(1)}\theta_1^{(3)}$, $\theta_1^{(1)}\theta_2^{(3)}$, $\theta_2^{(1)}\theta_1^{(3)}$, $\theta_2^{(1)}\theta_2^{(3)}$, $(\theta_1^{(2)})^2\theta_2^{(2)}$, $\theta_1^{(2)}(\theta_2^{(2)})^2$, $\theta_1^{(1)}\theta_2^{(1)}\theta_1^{(2)}$, $\theta_1^{(1)}\theta_2^{(1)}\theta_2^{(2)}$, $(\theta i^{\mathrm{AJ}})^{(2)}$, $(\theta_i^{\mathrm{AJ}})^{(3)}$, $(\theta_i^{\mathrm{AJ}})^{(4)}$ $(i = 1, 2)$
B_3	$(\theta_2^{(1)})^5$, $\theta_1^{(1)}(\theta_2^{(1)})^4$, $(\theta_1^{(1)})^2\theta_2^{(1)})^3$, $\theta_1^{(2)}(\theta_2^{(1)})^3$, $(\theta_2^{(1)})^3\theta_2^{(2)}$, $(\theta_1^{(2)})^2\theta_2^{(1)}$, $\theta_1^{(1)}(\theta_2^{(2)})^2$, $\theta_2^{(1)}(\theta_2^{(2)})^2$, $(\theta_1^{(1)})^2\theta_1^{(3)}$, $(\theta_2^{(1)})^2\theta_1^{(3)}$, $(\theta_1^{(1)})^2\theta_2^{(3)}$, $(\theta_2^{(1)})^2\theta_2^{(3)}$, $\theta_1^{(2)}\theta_1^{(3)}$, $\theta_2^{(2)}\theta_1^{(3)}$, $\theta_1^{(2)}\theta_2^{(3)}$, $\theta_2^{(2)}\theta_2^{(3)}$, $\theta_1^{(1)}\theta_1^{(2)}\theta_2^{(2)}$, $\theta_2^{(1)}\theta_1^{(2)}\theta_2^{(2)}$, $\theta_1^{(1)}\theta_2^{(1)}\theta_1^{(3)}$, $\theta_1^{(1)}\theta_2^{(1)}\theta_2^{(3)}$, $\theta_1^{(1)}(\theta_2^{(1)})^2\theta_1^{(2)}$, $(\theta_1^{(1)})^2\theta_2^{(1)}\theta_2^{(2)}$, $\theta_1^{(1)}(\theta_2^{(1)})^2\theta_2^{(2)}$, $(\theta_2^{(1)})^6$, $\theta_1^{(1)}(\theta_2^{(1)})^5$, $(\theta_1^{(1)})^4(\theta_2^{(1)})^2$, $(\theta_1^{(1)})^2(\theta_2^{(1)})^4$, $(\theta_1^{(1)})^3(\theta_2^{(1)})^3$, $\theta_1^{(2)}\ (\theta_2^{(1)})^4$, $(\theta_1^{(1)})^4\theta_2^{(2)}$, $(\theta_2^{(1)})^4\theta_2^{(2)}$, $(\theta_1^{(1)})^2(\theta_1^{(2)})^2$, $(\theta_2^{(1)})^2(\theta_1^{(2)})^2$, $(\theta_1^{(1)})^2(\theta_2^{(2)})^2$, $(\theta_2^{(1)})^2(\theta_2^{(2)})^2$, $(\theta_1^{(2)})^3$, $(\theta_2^{(2)})^3$, $(\theta_1^{(2)})^2\theta_2^{(2)}$, $\theta_1^{(2)}\ (\theta_2^{(2)})^2$, $(\theta_1^{(1)})^3\theta_1^{(3)}$, $(\theta_2^{(1)})^3\theta_1^{(3)}$, $(\theta_1^{(1)})^3\theta_2^{(3)}$, $(\theta_2^{(1)})^3\theta_2^{(3)}$, $(\theta_1^{(3)})^2$, $(\theta_2^{(3)})^2$, $\theta_1^{(3)}\theta_2^{(3)}$, $(\theta_1^{(1)})^3\theta_1^{(2)}\theta_2^{(1)}$, $\theta_1^{(1)}\theta_1^{(2)}\ (\theta_2^{(1)})^3$, $(\theta_1^{(1)})^3\theta_2^{(1)}\theta_2^{(2)}$, $\theta_1^{(1)}(\theta_2^{(1)})^3\theta_2^{(2)}$, $(\theta_1^{(1)})^2\theta_1^{(2)}(\theta_2^{(1)})^2$, $(\theta_1^{(1)})^2(\theta_2^{(1)})^2\theta_2^{(2)}$, $(\theta_1^{(1)})^2\theta_1^{(2)}\theta_2^{(2)}$, $(\theta_2^{(1)})^2\theta_1^{(2)}\theta_2^{(2)}$, $\theta_1^{(1)}\theta_2^{(1)}(\theta_1^{(2)})^2$, $\theta_1^{(1)}\theta_2^{(1)}(\theta_2^{(2)})^2$, $(\theta_1^{(1)})^2\theta_2^{(1)}\theta_1^{(3)}$, $\theta_1^{(1)}(\theta_2^{(1)})^2\theta_1^{(3)}$, $(\theta_1^{(1)})^2\theta_2^{(1)}\theta_2^{(3)}$, $\theta_1^{(1)}(\theta_2^{(1)})^2\theta_2^{(3)}$, $\theta_1^{(1)}\theta_1^{(2)}\theta_1^{(3)}$, $\theta_1^{(2)}\theta_1^{(3)}\theta_2^{(1)}$, $\theta_1^{(1)}\theta_1^{(3)}\theta_2^{(2)}$, $\theta_1^{(1)}\theta_1^{(2)}\theta_2^{(3)}$, $\theta_1^{(3)}\theta_2^{(1)}\theta_2^{(2)}$, $\theta_1^{(1)}\theta_2^{(2)}\theta_2^{(3)}$, $\theta_1^{(2)}\theta_2^{(1)}\theta_2^{(3)}$, $\theta_2^{(1)}\theta_2^{(2)}\theta_2^{(3)}$, $\theta_1^{(1)}\theta_2^{(1)}\theta_1^{(2)}\theta_2^{(2)}$, $(\theta_i^{\mathrm{AJ}})^{(4)}$, $(\theta_i^{\mathrm{AJ}})^{(5)}$, $(\theta_i^{\mathrm{AJ}})^{(6)}$, $(\theta_i^{\mathrm{AJ}})^{(4)}\theta_1^{(1)}$, $(\theta_i^{\mathrm{AJ}})^{(4)}\theta_2^{(1)}$, $(\theta_i^{\mathrm{AJ}})^{(4)}(\theta_i^{(1)})^{(2)}$, $(\theta_i^{\mathrm{AJ}})^{(4)}(\theta_2^{(1)})^2$, $(\theta_i^{\mathrm{AJ}})^{(4)}\theta_1^{(1)}\theta_1^{(1)}$, $(\theta_i^{\mathrm{AJ}})^{(5)}\theta_1^{(1)}$, $(\theta_i^{\mathrm{AJ}})^{(5)}\theta_2^{(1)}$, $(i = 1, 2)$

[a] For the sagittal plane.

terms of [ ] and $\theta_i^{(n)}$. Refer to Table 1 for A_1 and A_2.

(B) $[1, A_2, A_3]\cdot[\theta_i^{(4)}\cdot\dot{\theta}_j, \theta_i^{(4)}\cdot(\dot{\theta}_j)^2, \theta_i^{(4)}\cdot\dot{\theta}_1\cdot\dot{\theta}_2, \theta_i^{(4)}\cdot\ddot{\theta}_j, \theta_i^{(5)}\cdot\dot{\theta}_j]$ $(i, j = 1, 2)$
However, [ ].[ ] shows the product with each term of [ ]. Refer to Table 1 for A_2 and A_3.

Here, J_1 and J_2 are composed of terms; Eq. (15) is not substituted according to the standard, and $(\theta_i^{\mathrm{AJ}})^{(n)}$ $(n = 2, \ldots, 6)$. The composition terms of ${}_1h_{ik}$, ${}_2h_{ik}$, J_1 and J_2 are shown in Table 1.

3.3.2. A discretization of the movement time

Time t is dispersed to M divisions with equal intervals for the normalized movement time $[t_0, t_1, t_2, \ldots, t_m, \ldots, t_M]$ $(t_0 = 0, t_M = 1)$. Here, if a parameter a_{ik} expressing an optimal trajectory exists, the trajectory of Eq. (16) satisfies Eq. (11). That is, Eq. (16) satisfies the following equation.

$$\sum_{i=1}^{2}\sum_{k=0}^{K} {}_lh_{ik}(t_m, \theta_{1m}, \theta_{2m}, \dot{\theta}_{1m}, \dot{\theta}_{2m}, \ddot{\theta}_{1m}, \ddot{\theta}_{2m})a_{ik}$$

$$+J_l(t_m, \theta_{1m}, \theta_{2m}, \dot{\theta}_{1m}, \dot{\theta}_{2m}, \ldots, \theta_{1m}^{(3)}, \theta_{2m}^{(3)} = 0 \qquad (l = 1, 2, \quad 0 \le m \le M) \tag{17}$$

Here, the above equation is rearranged using ${}_lh_{ikm} = {}_lh_{ik}(t_m, \ldots)$ and $J_{lm} = J_l(t_m, \ldots)$ as follows.

$$\sum_{i=1}^{2}\sum_{k=0}^{K} {}_lh_{ikm}a_{ik} + J_{lm} = 0 \tag{18}$$

Eq. (18) holds for all discretization time values. Then, $2(M+1)$ linear equations of a_{ik} are derived. These equations are expressed as follows, in matrix form.

$$\begin{bmatrix} {}_1h_{100} & \cdots & {}_1h_{2K0} \\ \vdots & \ddots & \vdots \\ {}_1h_{10m} & \cdots & {}_1h_{2Km} \\ \vdots & \ddots & \vdots \\ {}_1h_{10M} & \cdots & {}_1h_{2KM} \\ {}_2h_{100} & \cdots & {}_2h_{2Ko} \\ \vdots & \ddots & \vdots \\ {}_2h_{10m} & \cdots & {}_2h_{2Km} \\ \vdots & \ddots & \vdots \\ {}_2h_{10M} & \cdots & {}_2h_{2KM} \end{bmatrix} \begin{bmatrix} a_{10} \\ a_{11} \\ \vdots \\ a_{1K} \\ a_{20} \\ \vdots \\ a_{2K} \end{bmatrix} + \begin{bmatrix} J_{10} \\ \vdots \\ J_{1m} \\ \vdots \\ J_{1M} \\ J_{20} \\ \vdots \\ J_{2m} \\ \vdots \\ J_{2M} \end{bmatrix} = \mathbf{0}$$

$$\mathbf{Ha} + \mathbf{J} = \mathbf{0}$$

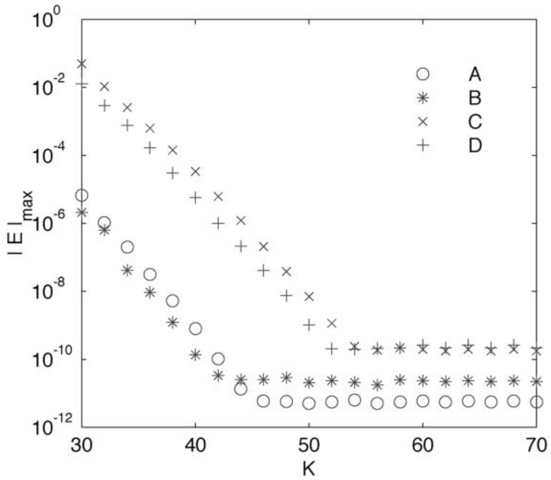

Fig. 1. Relationship between the number of parameters K and $|E|_{max}$. A, B, C, D: trajectories in Fig. 3.

Therefore,

$$\mathbf{a} = -\mathbf{H}^{\#}\mathbf{J} \quad (19)$$

Here, $\mathbf{H}^{\#}$ indicates a pseudo inverse matrix of $\mathbf{H}$. a_{ik} is estimated by an iterative calculation of the following method.

1. The initial value of parameter a_{ik} is set to 0, and joint angle trajectory θ_i is calculated from Eq. (15).
2. ${}_1h_{ikm}, {}_2h_{ikm}, J_{1m}$, and J_{2m} are calculated at every time t_m ($m = 0, 1, \ldots, M$).
3. a_{ik} is obtained from Eq. (19).
4. A new joint angle trajectory θ_i is calculated from Eq. (15) using a_{ik} computed in step 3.

Steps 2–4 are repeated until a_{ik} converges. In other words, in Eq. (19), let d ($d = 0, 1, 2, \ldots$) denote an index of the iterative calculation; the iterative calculation can be shown by the following equation.

$$\mathbf{a}^{d+1} = -\mathbf{H}(\mathbf{a}^d)^{\#}J(\mathbf{a}^d) \quad (20)$$

4. Numerical experiments of point-to-point movement on the horizontal and sagittal planes

The formation of minimum commanded torque change trajectories with the same starting point, final point, and motion duration as measured trajectories by Nakano et al. (1999) was carried out. The error of the Euler–Poisson equation was defined by the maximum value of the absolute value of the error, such as Eq. (21), to evaluate each predicted trajectory.

$$\max_{0 \le t_m \le 1} \sum_{i=1}^{2} |E_i^*(t_m) - E_i(t_m)| = |E|_{max} \quad (21)$$

Here, $E_i^*(t_m)$ shows the optimal value of $E_i(t_m)$. It is clear that $E_i^*(t) = 0$ ($0 \le t \le 1$) holds from Eq. (11). Whether the trajectory satisfies the Euler–Poisson equation can be judged according to the error definition. One thousand two hundred minimum commanded torque change trajectories were generated and measured by Nakano et al. (1999). First, the relationship between the number of parameters K and the error $|E|_{max}$ was examined in the proposed method. The value of K was changed (i.e. 30, 32, 34, …, 70). All of the initial values of a_{ik} were set to 0.

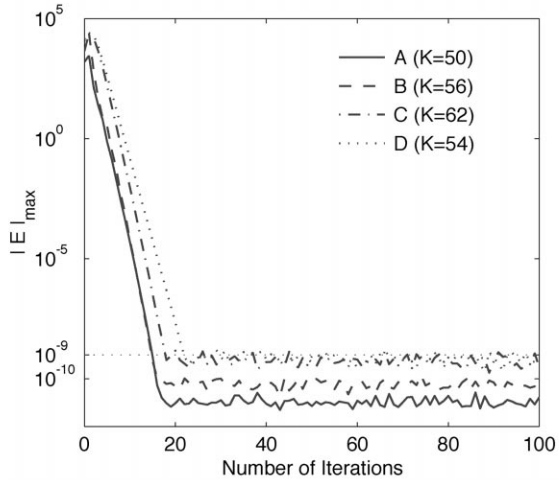

Fig. 2. Convergence of $|E|_{max}$. A, B, C, D: trajectories in Fig. 3.

Fig. 1 shows changes in error $|E|_{max}$ according to the number of parameters K. The horizontal axis shows the number of parameters K, and the vertical axis is $|E|_{max}$ calculated by Eq. (21). A, B, C, and D correspond to the four trajectories shown in Fig. 3. Though the error $|E|_{max}$ decreases as K increases, it converges near $K = 54$. The number of optimal parameters K differs according to the trajectory. Therefore, in the following, we use the number of parameters K that minimizes the error of $|E|_{max}$ for each trajectory.

Fig. 2. indicates the convergence of error $|E|_{max}$ in 100 times iterative calculations. The horizontal axis shows the iterative number of estimations of parameter a_{ik} and the vertical axis shows $|E|_{max}$ calculated by Eq. (21). $|E|_{max}$ for all trajectories converges to a small value below about 10^{-9}. It can therefore be said that the Euler–Poisson equations are satisfied with a high accuracy at every movement time of the trajectory. Moreover, the error clearly converges in a small number of iterative calculations, that is, about 20 times. Consequently, optimal trajectories can be obtained by the proposed method regardless of whether the trajectories can be solved by the Newton-like method or not.

The minimum commanded torque change trajectories on the horizontal plane obtained by the proposed method are shown in Fig. 3. The Y-axis of (a) is forward of the body, and the origin is the position of a shoulder. The optimal trajectories shown by the thick line cannot be obtained by the Newton-like method. Moreover, it can be understood that the features of human arm movements, that is hand

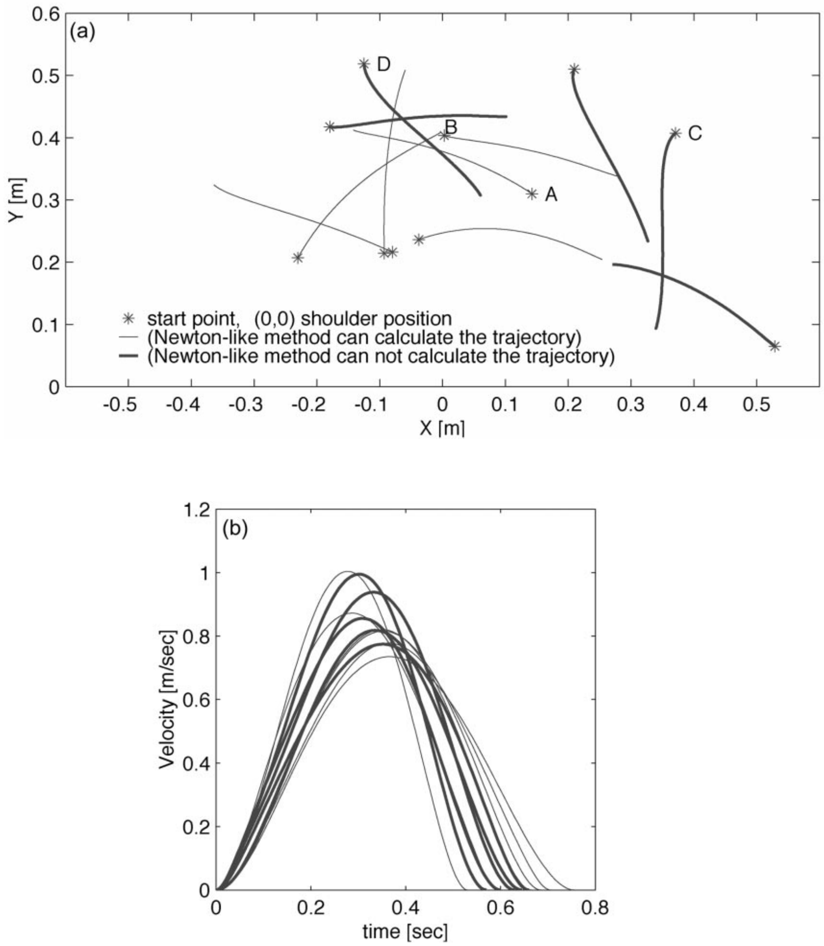

Fig. 3. Minimum commanded torque change trajectories calculated using the proposed method in the horizontal plane.

trajectories, are not straight lines, but gradually curved, and the velocity profiles each have a single peak and are reproduced well.

Table 2 indicates values of the object function (integration of the second power of the commanded torque change) for two trajectories solved by each method on the horizontal plane and the sagittal plane. It can be understood that the object function of the proposed method is smaller than or equal to the other methods for any case. Moreover, it can be confirmed that the proposed method can also obtain the converged trajectory solution, which is unable to be calculated by the Newton-like method.

To confirm how the proposed method and the Newton-like method satisfy the Euler–Poisson equations, E_1 and E_2 at every movement time were calculated.

Fig. 4 shows the absolute values of E_1 and E_2 at every time point for the proposed method and the Newton-like method. The horizontal axis indicates the normalized time, and the vertical axis is the absolute values of E_1 and E_2. It can be understood that the proposed method satisfies the Euler–Poisson equations better than the Newton-like method during the whole movement time.

5. Consideration

In experiments, we examined the validity of the minimum hand jerk criterion, minimum angle jerk criterion, minimum torque change criterion, and minimum commanded torque change criterion by comparing actual trajectories with trajectories predicted by these optimization criteria. For movements within the horizontal and sagittal planes, the minimum commanded torque change model was able to reproduce the spatial characteristics of measured trajectories. In this case, the magnitudes and directions of curvatures were better than those of the other three models. The minimum torque change model could reproduce neither the magnitudes nor the directions of curvatures. The minimum hand jerk model, which always predicts straight paths, showed a lack of correlation with the measured trajectories regarding the whole deviations.[1] Even though the minimum

[1] We investigated the trajectory curvatures quantified as an area bounded by a start-to-goal straight line and the hand path. This area was named the whole deviation. The whole deviation concerns the direction in which a trajectory had curved. If a trajectory had curved right relative to the vector from the start to the target, the area was designated positive; on the other hand, a trajectory that curved left was given a negative sign.

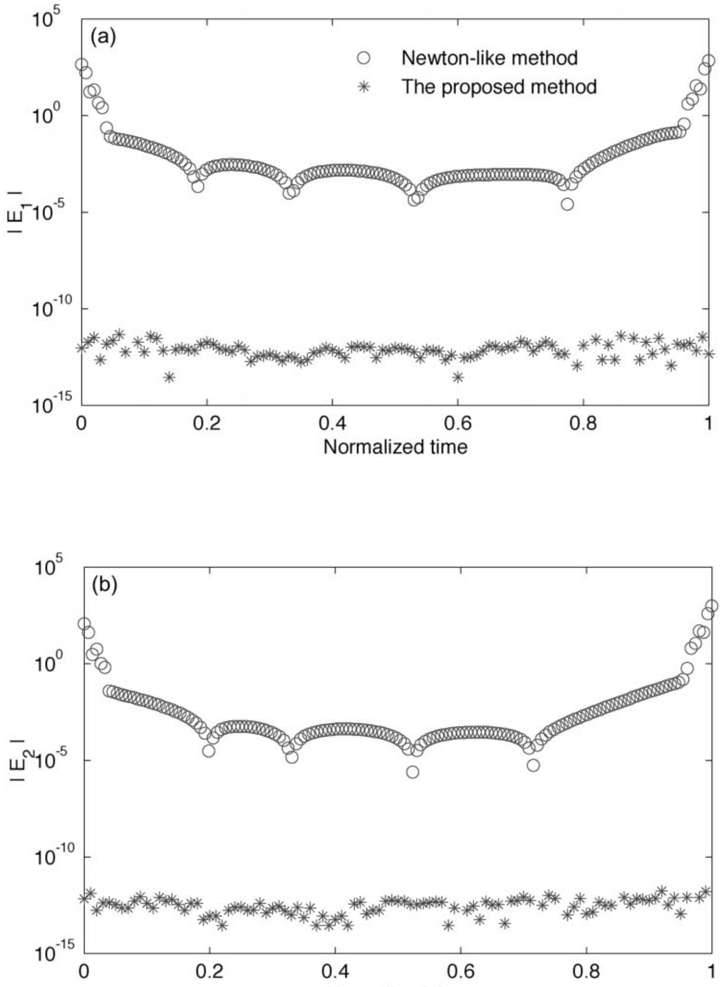

Fig. 4. Absolute values of E_1 and E_2 (trajectory A in Fig. 3. O: Newton-like method; *: the proposed method.

angle jerk model could explain the direction of the curvature, it predicted trajectories with obviously excessive curvatures (see Appendix B).

In previous studies, Hollerbach (1990); Osu, Uno, Koike, and Kawato (1997) suggested that planning in the joint space cannot explain a gently curved hand trajectory. As shown in Table 3, the slopes relating whole deviations of the minimum hand jerk and actual trajectories were zero (the mean error the slope was 1 in both planes). For minimum angle jerk trajectories, slopes were from 1.4 to 2.6 in the horizontal plane and from 1.3 to 1.5 in the sagittal plane (the mean error of the slope was 1 and 0.34, respectively). Hence, it can be considered that the minimum angle jerk model is quantitatively three times better than the minimum hand jerk model in the sagittal plane. Although the minimum angle jerk model has a qualitative weak point in predicting trajectories that are too curved, it is quantitatively a better model compared with the minimum hand jerk model. Accordingly, we demonstrated that it is impossible to completely reproduce actual data with trajectory planning in the kinematic space. As Flash (1990) pointed out, we confirmed that literal minimum torque change trajectories, computed without consideration of the viscosity, cannot reproduce any actual trajectory. Moreover, by the analysis of the trajectory, the velocity, and the acceleration and the torque, it was shown that the minimum commanded torque change criterion was able to explain the temporal features of actual hand trajectories best among the criteria. It can therefore be said that the minimum commanded torque change criterion is a better model than the other three criteria because the movement of the entire workspace can be explained in time and space. Moreover, the minimum commanded torque change criterion most similarly reproduced the feature of the measured trajectory in point-to-point movements on the sagittal plane. The whole deviations in minimum commanded torque change trajectories on the horizontal plane and the sagittal plane shown in Table 3 predict that the curvatures of the trajectories on both planes have almost the same tendency. Therefore, results such as a linear relation between the whole deviation of a trajectory measured in a horizontal plane and the whole deviation of a trajectory measured in a sagittal plane seem appropriate for the minimum commanded torque change criterion.

Table 2
Values of the performance index (the time integral of the square of the commanded torque change rate)

	1	2[a]
Horizontal plane		
The proposed method	33.4432	92.1030
Newton-like method	33.4432	–
Steepest descent method	33.4619	92.1660
Sagittal plane		
The proposed method	93.7844	40.3807
Newton-like method	93.7845	–
Steepest descent method	93.8458	40.3932

[a] –Shows that the method cannot calculate the optimal trajectory.

6. Summary

It was shown that the proposed method has the following advantages by numerical experiments. The trajectory obtained by the proposed method is similar to the trajectory of the mathematically guaranteed Newton-like method. An optimal trajectory, which cannot be obtained by the Newton-like method, is able to be calculated. Even if the value of the viscosity, which is one reason that a converged solution is unable to be obtained by the Newton-like method, is greatly changed, it can be confirmed that the proposed method is able to obtain an optimal solution. This was shown to obtain the converged solution in a very short period of time compared with the previous method. Though we searched for the most appropriate number of parameters K in the paper, a value of around $K = 60$ is sufficient as shown in Fig. 1. An optimal solution can be obtained by an iterative calculation of several ten times. The proposed method is a general method for a nonlinear, optimal problem. Therefore, the method can be applied to various optimization problems. However, an important remaining problem is to clarify the convergence conditions of the method theoretically.

Finally, we performed supplementary examinations of the experiments by Nakano et al. (1999). We recalculated the minimum commanded torque change trajectory using the proposed method; the same examinations as Nakano et al. (1999) were performed. As a result, it was reconfirmed that the measured trajectory was closest to the minimum commanded torque change trajectory, like the result by Nakano et al. (1999).

Acknowledgements

This study was performed through Special Coordination Funds for the promotion of Science and Technology of the Science and Technology Agency.

Appendix A

A.1. Jacobian polynomial

A Jacobian polynomial (Szego, 1975) is as follows. In general, there is family $(R_k|k = 0, 1, 2, \ldots)$ of polynomials defined by sections a and b.

$$(R_k, R_l)_w = \int_a^b R_k(x)R_l(x)w(x)\mathrm{d}x = 0 \qquad (\text{however, } k \neq l) \tag{22}$$

R_k and R_l to which Eq. (22) is satisfied are called an orthogonalization polynomial system concerning weight w in section a and in section b. This orthogonalization polynomial is obtained by the third recurrence formula (Szego, 1975). In particular, the following weight $w(x)$ is defined by section $(-1, 1)$.

$$w(x) = (1 + x)^{\alpha}(1 - x)^{\beta} \qquad (\alpha, \beta > -1) \tag{23}$$

Function $P_k^{(\alpha,\beta)}(x)$ $(k = 0, 1, \ldots)$, which is orthogonal concerning Eq. (23), is a Jacobian polynomial. Here,

$$(P_k^{(\alpha,\beta)}, P_l^{(\alpha,\beta)})_w = \int_{-1}^{1} P_k^{(\alpha,\beta)}(x)(w(x))^{1/2}P_l^{(\alpha,\beta)}(x)(w(x))^{1/2}\mathrm{d}x \tag{24}$$

Table 3
Results of a t-test for measured whole deviations and simulated whole deviations. (r: correlation coefficient; t: t values; df: degrees of freedom; $*p < 0.05$; $**p < 0.01$; HJ: minimum hand jerk criterion; AJ: minimum angle jerk criterion; TC: minimum torque change criterion; CTC: minimum commanded torque change criterion)

Subjects	MM				YS				TT			
Models	r	t	df	Slope	r	t	df	Slope	r	t	df	Slope
A Horizontal plane												
HJ	0	–	–	0	0	–	–	0	0	–	–	0
AJ	0.727	14.56**	189	1.933	0.680	12.62**	185	2.645	0.835	20.17**	177	1.440
TC	− 0.365	5.39**	189	− 0.943	− 0.298	4.25**	185	− 0.993	− 0.363	5.18**	177	− 0.618
CTC	0.798	18.18**	189	0.819	0.691	12.99**	185	1.302	0.654	11.50**	177	0.485
B Sagittal plane												
HJ	0	–	–	0	0	–	–	0	0	–	–	0
AJ	0.751	15.12**	177	1.487	0.733	14.20**	174	1.278	0.788	17.04**	177	1.265
TC	− 0.400	5.81**	177	− 0.485	− 0.322	4.49**	174	− 0.302	− 0.358	5.11**	177	− 0.375
CTC	0.777	16.44**	177	0.894	0.829	19.54**	174	0.900	0.771	16.12**	177	0.700

Table 4
Results of Bonferroni's *t*-test for the mean squared errors of measured trajectories and simulated trajectories. Pairwise comparisons were carried out for four models. *t*: *t* values; df: degrees of freedom; $*p < 0.05$; $**p < 0.01$; HJ: minimum hand jerk criterion; AJ: minimum angle jerk criterion; TC: minimum torque change criterion; CTC: minimum commanded torque change criterion. The model of which the amount of mean squared errors was significantly small is shown to the right of the level of significance)

Subjects		MM			YS			TT		
		t	df		*t*	df		*t*	df	
A Horizontal plane										
HJ–AJ	Trajectory	9.35**	190	HJ	13.54**	186	HJ	3.25**	178	HJ
	Velocity	12.02**	190	HJ	17.00**	186	HJ	6.42**	178	HJ
	Acceleration	13.32**	190	HJ	17.50**	186	HJ	8.76**	178	HJ
	Torque	2.78**	190	HJ	5.60**	186	HJ	0.83	178	
HJ–TC	Trajectory	11.80**	190	HJ	7.66**	186	HJ	10.28**	178	HJ
	Velocity	12.60**	190	HJ	8.35**	186	HJ	10.67**	178	HJ
	Acceleration	13.27**	190	HJ	8.83**	186	HJ	10.55**	178	HJ
	Torque	1.09	190		2.87**	186	HJ	1.18	178	
HJ–CTC	Trajectory	4.07**	190	CTC	0.17	186		4.58**	178	CTC
	Velocity	4.00**	190	CTC	0.93	186		5.66**	178	CTC
	Acceleration	0.59	190		0.71	186		3.99**	178	CTC
	Torque	5.16**	190	CTC	5.04**	186	CTC	5.09**	178	CTC
AJ–TC	Trajectory	7.24**	190	AJ	0.75	186		8.30**	178	AJ
	Velocity	6.06**	190	AJ	1.50	186		7.11**	178	AJ
	Acceleration	4.81**	190	AJ	3.57**	186	TC	5.79**	178	AJ
	Torque	5.08**	190	TC	10.66**	186	TC	2.78**	178	TC
AJ–CTC	Trajectory	12.42**	190	CTC	14.22**	186	CTC	6.02**	178	CTC
	Velocity	15.27**	190	CTC	17.60**	186	CTC	9.51**	178	CTC
	Acceleration	14.67**	190	CTC	16.79**	186	CTC	10.45**	178	CTC
	Torque	8.45**	190	CTC	12.53**	186	CTC	7.15**	178	CTC
TC–CTC	Trajectory	14.00**	190	CTC	7.77**	186	CTC	13.12**	178	CTC
	Velocity	14.84**	190	CTC	8.96**	186	CTC	13.80**	178	CTC
	Acceleration	14.63**	190	CTC	9.13**	186	CTC	12.92**	178	CTC
	Torque	12.80**	190	CTC	6.82**	186	CTC	12.54**	178	CTC
B Sagittal plane										
HJ–AJ	Trajectory	4.38**	178	HJ	2.67**	175	HJ	2.47**	178	HJ
	Velocity	5.79**	178	HJ	3.80**	175	HJ	3.53**	178	HJ
	Acceleration	6.28**	178	HJ	4.55**	175	HJ	3.98**	178	HJ
	Torque	1.71	178		2.65**	175	HJ	0.52	178	
HJ–TC	Trajectory	6.71**	178	HJ	6.60**	175	HJ	6.38**	178	HJ
	Velocity	6.80**	178	HJ	6.75**	175	HJ	6.60**	178	HJ
	Acceleration	6.94**	178	HJ	6.93**	175	HJ	6.79**	178	HJ
	Torque	1.16	178		1.55	175		0.35	178	
HJ–CTC	Trajectory	2.79**	178	CTC	3.60**	175	CTC	3.88**	178	CTC
	Velocity	0.69	178		2.19*	175	CTC	3.00**	178	CTC
	Acceleration	2.59*	178	HJ	0.57	175		0.66	178	
	Torque	1.68	178		1.34	175		3.47**	178	CTC
AJ–TC	Trajectory	3.46**	178	AJ	3.57**	175	AJ	3.78**	178	AJ
	Velocity	2.41*	178	AJ	2.94**	175	AJ	3.39**	178	AJ
	Acceleration	1.68	178		2.52*	175	AJ	3.33**	178	AJ
	Torque	0.68	178		1.63	175		0.20	178	
AJ–CTC	Trajectory	6.87**	178	CTC	5.83**	175	CTC	5.87**	178	CTC
	Velocity	6.90**	178	CTC	5.98**	175	CTC	6.03**	178	CTC
	Acceleration	5.26**	178	CTC	4.60**	175	CTC	4.50**	178	CTC
	Torque	4.09**	178	CTC	3.88**	175	CTC	3.89**	178	CTC
TC–CTC	Trajectory	7.89**	178	CTC	7.28**	175	CTC	7.89**	178	CTC
	Velocity	6.93**	178	CTC	6.74**	175	CTC	7.43**	178	CTC
	Acceleration	5.44**	178	CTC	5.51**	175	CTC	6.53**	178	CTC
	Torque	5.43**	178	CTC	5.19**	175	CTC	6.31**	178	CTC

Consider the following equation.

$$w(x) = (1+x)^6(1-x)^6$$
$$= \left\{(1+x)^6(1-x)^6\right\}^{1/2}\left\{(1+x)^6(1-x)^6\right\}^{1/2}$$
$$= (1+x)^3(1-x)^3(1+x)^3(1-x)^3 \quad (25)$$

$Q_k(x) = (1+x)^3(1-x)^3 P_k^{(6,6)}(x)$ is as follows at both ends of section 1 and -1.

$$Q_k(-1) = Q_k(1) = 0, \qquad \left.\frac{dQ_k(x)}{dx}\right|_{x=-1} = \left.\frac{dQ_k(x)}{dx}\right|_{x=1} = 0,$$
$$\left.\frac{d^2Q_k(x)}{dx^2}\right|_{x=-1} = \left.\frac{d^2Q_k(x)}{dx^2}\right|_{x=1} = 0 \quad (26)$$

Here, by the coordinate transformation of $t = (x+1)/2$, $\tilde{Q}_k(t) = 64t^3(1-t)^3\tilde{P}_k^{(6,6)}(t)$ is obtained.

A.2. Jacobian polynomial of k + 1

The following Jacobian polynomial of $k+1$ is given as follows, where the coefficient of the highest degree is assumed as 1,

$$P_0^{(6,6)}(x) = 1$$

$$P_1^{(6,6)} = x$$

$$P_2^{(6,6)}(x) = x^2 - \frac{1}{15}$$

$$\vdots \quad \vdots$$

$$P_{k+1}^{(6,6)}(x) = (x - \alpha_k)P_k^{(6,6)}(x) - \beta_k P_{k-1}^{(6,6)}(x)$$

$$\alpha_k = \frac{(xP_k^{(6,6)}(x), P_k^{(6,6)}(x))_w}{(P_k^{(6,6)}(x), P_k^{(6,6)}(x))_w} \qquad (k = 0, 1, 2, \ldots)$$

$$\beta_k = \frac{(P_k^{(6,6)}(x), P_k^{(6,6)}(x))_w}{(P_{k-1}^{(6,6)}(x), P_{k-1}^{(6,6)}(x))_w} \qquad (k = 1, 2, \ldots)$$

However, $P_{-1}^{(6,6)}(x) = 0$.

Appendix B. Quantitative examination of the spatial and time features of trajectories

We recalculated the minimum commanded torque change trajectory using the proposed method, and performed the same examinations as Nakano et al. (1999). Compared with the actual trajectories, many of the minimum angle jerk trajectories and minimum torque change trajectories are largely curved towards the outside and inside of the body, respectively. As a result of the analysis, we plotted the correlations between the whole deviations of measured and predicted trajectories. Table 3 summarizes the correlation coefficients, the results of a test on the correlations, and the slopes of the regression lines of all of the subjects in the horizontal and sagittal planes. All of the minimum hand jerk trajectories were straight; this indicated that they were not correlated with those of actual trajectories. The minimum angle jerk trajectories were curved more than the actual trajectories. Most of the whole deviations of the minimum torque change trajectories had negative correlations to those of actual trajectories, and the correlation coefficients were low. The whole deviations of the minimum commanded torque change trajectories were smaller than, or approximately the same as, those of actual trajectories, and the correlation coefficients were high.

As a result of the second analysis, we carried out a *t*-test for the MSEs of the position, velocity, acceleration, and torque of all of the trajectories measured in both planes. In 72 total comparisons between the minimum commanded torque change model and the other three models, and with the four characteristics, three subjects, and two planes ($3 \times 4 \times 3 \times 2$), the MSEs of the minimum commanded torque change model for 62 comparisons were smaller (significiantly smaller, $P < 0.05$) (Table 4). We roughly summarized that the minimum commanded torque change model was the best one for the MSEs.

References

Abend, W., Bizzi, E., & Morasso, P. (1982). Human trajectory formation. *Brain*, *105*, 331–348.

Akazawa, K. (1994). Modulation and adaptation of mechanical properties of mammalian skeletal muscle. In Y. Hirasawa, C. B. Sledge & S. -Y. Wood, *Clinical biomechanics and related research* (pp. 217–227). Tokyo: Springer-Verlag.

Bizzi, E., Accornero, N., Chapple, W., & Hogan, N. (1984). Posture control and trajectory formation during arm movement. *Journal of Neuroscience*, *4*, 2738–2744.

Flash, T. (1990). The organization of human arm trajectory control. In J. M. Winters & S. -Y. Woo, *Multiple muscle systems* (pp. 282–301). New York: Springer-Verlag.

Flash, T., & Hogan, N. (1985). The coordination of arm movements; an experimentally confirmed mathematical model. *Journal of Neuroscience*, *5*, 1688–1703.

Gomi, H., & Osu, R. (1998). Task dependent viscoelasticity of human multijoint-arm and its spatial characteristics for interaction with environments. *Journal of Neuroscience*, *18* (21), 8965–8978.

Hollerbach, J. M. (1990). Planning of arm movement. In D. N. Osherson, S. M. Kosslyn & J. M. Hollerbach, *Visual cognition and action* (pp. 183–211). Cambridge, MA: MIT Press.

Kawato, M. (1992). Optimization and learning in neural networks for formation and control of coordinated movement. In D. E. Meyer & S. Kornblum, *Attention and performance XIV* (pp. 821–849). Cambridge, MA: MIT Press.

Kawato, M. (1996). Trajectory formation in arm movements: minimization principles and procedures. In H. N. Zelaznik, *Advances in motor learning and control* (pp. 225–259). Champaign, IL: Human Kinetics Publishers.

Koike, Y., & Kawato, M. (1995). Estimation of dynamic joint torques and trajectory formation from surface electromyography signals using a neural network model. *Biological Cybernetics*, *73*, 291–300.

Nakano, E., Imamizu, H., Osu, R., Uno, Y., Gomi, H., Yoshioka, T., & Kawato, M. (1999). Quantitative examinations of internal representations for arm trajectory planning: minimum commanded torque change model. *Journal of Neurophysiology*, *81* (5), 2140–2155.

Osu, R., Uno, K., Koike, Y., & Kawato, M. (1997). Possible examination of trajectory curvature in multijoint arm movement. *Journal of Experimental Psychology: Human Perception and Performance*, *23* (3), 890–913.

Rosenbaum, D. A., Loukopoulos, L. D., Meulenbroek, R. G., Vaughan, J., & Engelbrecht, S. E. (1995). Planning reaches by evaluating stored posture. *Psychological Review*, *102*, 28–67.

Sakuraba, H., Osu, R., Nakano, R., Wada, Y., & Kawato, M. (2000). An explanation for the feature of a hand trajectory controlled by an imperfect inverse dynamics model. *IEICE*, J83-D-II(2), 784–794 (in Japanese).

Szego, G. (1975). *Orthogonal polynomials*, (4th ed).

Uno, Y., Kawato, M., & Suzuki, R. (1989). Formation and control of optimal trajectory in human arm movement—minimum torque-change model. *Biological Cybernetics*, *61*, 89–101.